








## ARTICLE

# Enzymatic hydrolysis of bacterial cellulose in the presence of a non-catalytic cerato-platanin protein

Cesare Rovera<sup>1</sup>  | Simone Luti<sup>2</sup>  | Luigia Pazzagli<sup>2</sup>  | Ellen L. Heeley<sup>3</sup>  |  
Chaoying Wan<sup>4</sup>  | Diego Romano<sup>1,5</sup>  | Stefano Farris<sup>1,5</sup> 

<sup>1</sup>DeFENS, Department of Food, Environmental and Nutritional Sciences, University of Milan, Milan, Italy

<sup>2</sup>Department of Biomedical, Experimental and Clinical Sciences, University of Florence, Florence, Italy

<sup>3</sup>School of Life, Health and Chemical Sciences, The Open University, Walton Hall, Milton Keynes, UK

<sup>4</sup>International Institute for Nanocomposites Manufacturing (IINM), WMG, University of Warwick, Coventry, UK

<sup>5</sup>INSTM, National Consortium of Materials Science and Technology, Local Unit University of Milan, Milan, Italy

## Correspondence

Stefano Farris, Department of Food, Environmental and Nutritional Sciences, University of Milan, via Celoria 2 – I-20133 Milan, Italy.  
Email: stefano.farris@unimi.it

Simone Luti, Department of Biomedical, Experimental and Clinical Sciences "Mario Serio", University of Florence, Viale G. B. Morgagni 50 – I-50134 Florence, Italy.  
Email: simone.luti@unifi.it

## Abstract

In this work, the effect of an expansin-like cerato-platanin (CP) protein as a pre-treatment for the enzymatic hydrolysis of bacterial cellulose (BC) is investigated. To this scope, cellulases from *Trichoderma reesei* are used as hydrolyzing agent using different enzyme/BC formulations. Turbidity experiments reveal that for the higher enzyme concentrations (formulations 0.5:1 and 1:1) the enzymatic hydrolysis of BC show similar hydrolysis kinetics and is not dependent of the CP. However, at higher BC concentrations (formulations 0.25:1 and 0.33:1), the hydrolysis of BC is hindered by the non-catalytic protein, as confirmed by the lower content of cellobiose and glucose in the presence of CP. Light scattering experiments show that the addition of CP led to an increase of the BC particle size from (445–630 nm) to (890–1.26 μm) for the formulation 1:1, which is also corroborated by atomic force microscopy and transmission electron microscopy analyses. These results suggest that CP did not positively affect the hydrolysis of BC, in contrast to what was previously observed for plant-derived cellulose. This work for the first time investigates the anomalous behavior of cerato platanin family members with regard to its loosening activity on the structure of bacterial cellulose.

## KEYWORDS

biomaterials, enzymatic hydrolysis, packaging, proteins

## 1 | INTRODUCTION

Cerato-platanins are proteins produced exclusively by fungi and belong to a protein family discovered 20 years ago (Cerato platanin family—CPF).<sup>1</sup> They are the most abundant proteins found in the cultural filtrate of several phytopathogenic fungi, in which they play a role in plant-pathogen interactions.<sup>2–4</sup> They are secreted during

infection, and it has been hypothesized that they can facilitate pathogen penetration through their polysaccharides' weakening activity.<sup>5</sup> To date, why fungi produce cerato-platanin family proteins is still unknown: they are presents in the fungal cell walls suggesting that they may be involved in fungal growth and development possibly acting as expansins in the fungal cell wall.<sup>6</sup> On the other hand, several experimental data indicated that they are

This is an open access article under the terms of the Creative Commons Attribution License, which permits use, distribution and reproduction in any medium, provided the original work is properly cited.

© 2021 The Authors. *Journal of Applied Polymer Science* published by Wiley Periodicals LLC.

secreted in different conditions and that fungal mutant with impaired expression cerato-platanins reduced their pathogenicity supporting a role for cerato-platanins in virulence.<sup>2</sup>

From a biochemical point of view, the main distinctive trait of CPF members is the presence of four cysteines in a conserved region forming two disulfide bridges, which give these proteins extreme stability at high temperatures and in acidic media.<sup>2,7</sup> They are characterized by a single domain of 105–134 amino acids with a double  $\psi\beta$ -barrel fold, similar to that of plant and bacterial expansins known to be involved in wall-loosening activity.<sup>7,8</sup> In particular, expansin-like activity on cellulosic materials has been described as for *C. platani* cerato-platanin, the first identified member of the family, along with *M. perniciosae* MpCP2, and *F. graminearum* FgCPPs.<sup>8–10</sup> These proteins can loosen plant cellulose in a concentration-dependent manner through a non-lytic mechanism, making them particularly interesting for biotechnological uses. By site-directed mutagenesis experiments has been demonstrated that the expansin-like activity of CP depends both on net charge of the protein surface and ability to weakly bind cellulose.<sup>11,12</sup> Interestingly, it has been shown recently that members of CPF are able to enhance fungal cellulase activity on different substrates, such as plant cellulose and plant cellulose derivatives (e.g., filter paper and carboxymethyl cellulose).<sup>10,12</sup> Moreover, recently it has been demonstrated that the ThCP from *T. harzianum* is able to valorize lignocellulosic Agri-food Wastes.<sup>13</sup>

Bacterial cellulose (BC) produced by acetic bacteria has gained much attention due to its outstanding properties in fabricating multi-functional nano-biomaterials.<sup>14</sup> When compared with other conventional natural or synthesized counterparts, BC performs better in areas such as biomedicine, functional devices, water treatment, nanofillers, etc., for its superior chemical purity, crystallinity, biocompatibility, and ultrafine network architecture.<sup>15,16</sup> Cellulose produced by *Komagataeibacter xylinum* (*Acetobacteraceae* family), in particular, is devoid of other components found in cellulose derived from plants, such as lignin, hemicellulose, and pectin. In addition, the spatial arrangement of the pre-microfibril aggregation provides a high crystallinity up to 84%–89%,<sup>17</sup> while the data varies from 40% to 60% for plant cellulose.<sup>18</sup> Furthermore, BC isolation and purification are relatively simple in that they do not require energy- or chemical-intensive processes.<sup>19</sup>

Not only native BC, but also BC derivatives have found widespread use for several applications. Bacterial cellulose nanocrystals (BCNCs), in particular, obtained from a top-down process (e.g., physical, chemical, or physicochemical processes) of BC, have gathered much

attention in the materials community that does not appear to be relenting.<sup>20,21</sup> The size of cellulose nanocrystals depends on the source as well as on the hydrolysis conditions. The high rigidity of the cellulose nanocrystals combined with the high tensile strength ( $\sim 7.6$  GPa),<sup>22</sup> high length-diameter ratio ( $L/d - \text{nm}$ : 2–100),<sup>23</sup> relatively high specific surface area ( $\sim 13 \text{ m}^2 \text{ g}^{-1}$ ),<sup>24</sup> and biodegradability, make the BCNCs an excellent alternative to the reinforcing inorganic fillers (e.g., clays) used in polymeric materials.

The most commonly employed method to obtain cellulose nanocrystals from the parental macro-sized cellulose fibers is acid hydrolysis, which commonly uses sulfuric and hydrochloric acids.<sup>21</sup> As an alternative route, the enzymatic hydrolysis of cellulosic materials mediated by cellulases has shown the potential to achieve higher yields, higher selectivity, lower energy costs, and milder operating conditions than chemical processes. However, extended hydrolysis time and a relatively high number of enzymes make the overall process economically unviable.<sup>25</sup> The degradation kinetics of the amorphous regions of cellulose by cellulases depends, among other factors, on the degree of crystallinity of the substrate; therefore, finding a method that can somehow limit the shielding effect of the crystalline phase is crucial for a rapid enzymatic attack. To make the amorphous regions readily available, several pre-treatments have been proposed, such as catalyzed and uncatalyzed steam explosion, liquid hot water pre-treatment, mechanical comminution, high-energy radiation, acid, alkaline, ammonia fiber/freeze explosion, ionic liquids, and biological pre-treatments.<sup>26</sup> Among the biological pre-treatments, the use of proteins (e.g., plant expansins) able to loosen and disrupt the non-covalent bonding networks of polysaccharide cell walls represents one of the most attractive ways to reduce manufacturing costs by increasing the activity of cellulolytic enzymes. Moreover, the addition of cellulose-binding domains (CBDs) from cellulases in cellulose-rich materials, were successfully used as a biological pre-treatment step in the glucose conversion process of the fibrous substrate, making it less recalcitrant for the subsequent enzymatic hydrolysis.<sup>27</sup> Similar results were also obtained combining the effect of white rot fungi and liquid hot water as a biomass pre-treatment.<sup>28</sup> As reported in literature, when compared with the other cited methods (e.g., high energy radiation, alkaline or acid methods), biological pre-treatments exhibit extra benefits being considered both an environmental friendly (mainly due to the limited energy consumption) and an economically viable process.<sup>29</sup>

In this work, we tested the expansin-like activity of CP on the enzymatic hydrolysis of BC mediated by the cellulases from *Trichoderma reesei*. The goal of this

study is to explore the use of CP as a pre-treatment to promote the overall hydrolysis kinetics of BC. The effect of the CP was assessed by comparing the physico-chemical properties of raw BC with the newly formed BCNCs in terms of size distribution, sugar content, and structural organization. To the best of our knowledge, the assessment of the expansin-like activity of ceratoplatanins on cellulose of bacterial origin has never been reported before.

## 2 | MATERIALS AND METHODS

### 2.1 | Cerato-platanin production and purification

CP purification was performed as reported in Luti et al. in 2016,<sup>30</sup> with some modifications. Briefly, the protein was produced in *P. pastoris*, recovered from the cultural filtrate, and loaded into a HiLoad 16/600 Superdex 200 pg column through an FPLC system (AKTA Pure, GE), using sodium acetate 50 mM pH 5.0 and NaCl 150 mM as buffers. This method allows the purification of about 200 mg of pure protein starting from 1 L of cultured medium.

### 2.2 | Production of the macro-sized bacterial cellulose

BC was produced by static fermentation using *Komagataeibacter sucrofermentans* DSM 15973 (Leibniz Institute DSMZ-German Collection of Microorganisms and Cell Cultures, Braunschweig Germany) in  $630 \times 430 \times 115 \text{ mm}^3$  rectangular polypropylene trays: 4 L of Hestrin and Schramm (HS) medium (glucose:  $20 \text{ g L}^{-1}$ ; peptone:  $5 \text{ g L}^{-1}$ ; yeast extract:  $5 \text{ g L}^{-1}$ ;  $\text{Na}_2\text{HPO}_4$ :  $2.7 \text{ g L}^{-1}$ ; citric acid:  $1.15 \text{ g L}^{-1}$ ; pH 6.0) were inoculated with 0.5 L of pre-culture (HS medium, 2-L Erlenmeyer flask, growth for 48 h at  $30^\circ\text{C}$ , 150 rpm). After 7 days at  $30^\circ\text{C}$ , the resulting BC pellicles were removed from the cultural medium, washed with deionized water, and boiled in an alkaline solution (NaOH 1 M) for 30 min to remove the residual bacterial cells. After extensive washing with distilled water until neutrality, the cellulosic material was homogenized for 15 min with an Ultra-turrax® T25 Basic homogenizer (Ika-Werke, Stanfen, Germany) at 12,000 rpm and finally freeze-dried at  $-55^\circ\text{C}$  and 0.63 mbar for 24 h using an ALPHA 1–2 LDplus freeze dryer (Martin Christ, Osterode am Harz, Germany). All the chemicals involved in the production of bacterial cellulose were purchased from Sigma-Aldrich (Sigma Aldrich, Milano).

### 2.3 | Enzymatic hydrolysis of bacterial cellulose

To evaluate the boosting effect of the CP on the degradation of BC, the enzymatic hydrolysis of the cellulosic substrate was performed using cellulase enzyme with and without the addition of the non-catalytic CP. A stock of BC in water was prepared by adding 12 g of freeze-dried BC to 88 ml of distilled water. Then, 1 g of the dispersion was added to 30 ml of sodium acetate/acetic acid buffer solution, 0.1 M, pH 5. The dispersion was homogenized using an Ultra-turrax® T25 Basic homogenizer (Ika-Werke, Stanfen, Germany) at 8000 rpm for 5 min and then kept in an incubator at  $55 \pm 1^\circ\text{C}$  overnight to facilitate the diffusion of water molecules into the cellulosic network, hence promoting an even degradation of the amorphous regions upon adding the enzymatic mixture. When the CP was added, the same procedure as above was employed, with the exception of the amounts used. In particular, the initial dispersion of BC was prepared by adding 12 g of freeze-dried BC to 88 ml of distilled water. Then, 1 g of the stock dispersion was added to 24.17 ml of sodium acetate/acetic acid buffer solution, 0.1 M, pH 5 and 5.83 ml of CP buffer solution containing the non-catalytic protein at a final concentration of  $153 \mu\text{M}$ . As reported above, the dispersion was then kept in an incubator at  $55 \pm 1^\circ\text{C}$  overnight (18 h) before the addition of the enzyme.

The enzymatic hydrolysis was performed using cellulase from *Trichoderma reesei* (ATCC26921) (Sigma Aldrich, Milano). The lyophilized powder (enzymatic activity  $\sim 6.5 \text{ U mg}^{-1} \text{ solid}$ ) was dissolved in water to a stock concentration of  $5 \text{ mg ml}^{-1}$  ( $\sim 100 \mu\text{M}$ ) and the digestion was performed at  $55 \pm 1^\circ\text{C}$  for a minimum of 2 h and a maximum of 166 h both with and without CP, using an initial stock solution of the enzyme in water ( $5 \text{ mg ml}^{-1}$ ). As previously reported by Rovera et al. in 2018, cellulase from *Trichoderma reesei* includes a variety of enzymes that attach selectively the cellulose binding sites among cellulosic backbone. In particular, (i) endo-1,4- $\beta$ -glucanases (EGs) enzyme, which target cellulose chains in random locations away from the chain ends, quickly degrade the amorphous regions of the cellulose chains to produce smaller cellulose fragments, (ii) exoglucanases or cellobiohydrolases (CBHs) enzyme, which degrade cellulose by splitting off molecules from both ends of the chain, thus producing cellobiose dimers, included short crystalline regions of cellulose and (iii)  $\beta$ -glucosidases enzyme, which hydrolyze the cellobiose units that are produced during the EG and CBH attacks, turning them into glucose.<sup>25</sup> Four different mixtures were eventually prepared (Table 2) by varying the amount of the enzyme and keeping the amount of BC and CP buffer

solution (where used) constant throughout the experiments (2.74 g of a BC dispersion with a concentration of ~15 wt%). For the experiments with CP, the amount of this protein was kept at 153  $\mu\text{M}$  so to maintain constant the ratio between CP and BC. After the enzymatic hydrolysis (both with and without the addition of CP), BCNCs were left in the original enzyme-rich water-based dispersions at room temperature for 24 h before further characterization.

## 2.4 | Enzymatic hydrolysis kinetics

The evolution of the enzymatic hydrolysis was monitored at 2-h intervals in turbidity experiments,<sup>25</sup> over a temporal window of 166 h. Spectrophotometric measurements were performed using a Lambda 25 spectrophotometer (Perkin Elmer, Waltham, MA) at wavelengths between 380 and 800 nm in transmittance mode. For each sample, the area under the transmittance spectrum was calculated by means of PerkinElmerUV WinLab software (version 6.0.4.0738) and plotted over time.

## 2.5 | High-performance liquid chromatography

Cellobiose and glucose, as possible ultimate products of the enzymatic process, were quantified using high-performance liquid chromatography (HPLC). The supernatant obtained from the centrifugation of the enzyme/BC mixture (which was itself obtained after 166 h of hydrolysis) underwent an initial centrifugation at 4000 rpm ( $2630 \times g$ ) for 15 min. Subsequently, an additional centrifugation was performed at 14,000 rpm ( $9205 \times g$ ) for 5 min, in order to completely remove the residual particles that were still present in the supernatant. The HPLC analysis was performed using a Merck Hitachi L-7100 system with an Aminex HPX-87P column ( $300 \times 7.8$  mm; Biorad Laboratories, Hercules, CA) and an evaporative light-scattering detector (Sedex 75; Sedere, Alfortville, France; conditions: He 3.5 bar,  $50^\circ\text{C}$ ). The analysis was carried out at  $60^\circ\text{C}$  using water ( $0.5 \text{ ml min}^{-1}$ ) as the eluent.

## 2.6 | Particle size

Information on the size distribution of BCNCs was obtained through photon correlation spectroscopy using a dynamic light-scattering Nanotracs Flex in-situ analyzer (Microtrac Inc., USA). Analyses were carried out at  $25^\circ\text{C}$ , with a stabilization time of 60 s, and using the viscosity

of water ( $\nu = 0.8872 \text{ cP}$ ) and refractive index ( $n = 1.330$ ) as reference values. The size distribution of the particles was calculated using the software Flex (Microtrac Inc., USA) and supported by the nonnegative least squares algorithm.

## 2.7 | Atomic force microscopy

AFM experiments were performed using a Nanoscope V Multimode (Bruker, Karlsruhe, Germany) in tapping mode after dropping 10  $\mu\text{l}$  of 1:10 diluted BCNC dispersion onto a mica substrate. The images were collected at a resolution of  $512 \times 512$  pixels using silicon tips (force constant,  $3 \text{ N m}^{-1}$ ; resonance frequency,  $\sim 75 \text{ kHz}$ ).

## 2.8 | Transmission electron microscopy

A transmission electron microscope (TEM) (LEO 912 AB energy-filtering, operating at 80 kV; Zeiss, Oberkochen, Germany) was used to capture images of the BCNCs at  $100,000\times$  magnification. Digital images were recorded with a ProScan 1 K Slow-Scan CCD camera (ProScan, Scheuring, Germany). Samples for the TEM analyses were prepared according to the negative staining technique by drop-casting a few microliters of dispersion onto a glow-discharged Formvar-coated Cu grid (400-mesh) and letting the samples rest for 1–2 min, then blotting the excess of suspension and contrasting with uranyl acetate.

## 2.9 | X-ray diffraction

Information about the crystalline polymorphs and crystallinity index (CI) of both cellulosic substrates, that is, BC and the control, a Whatman grade 3MM filter paper (Whatman-GE Healthcare, Maidstone, UK), was gathered using wide-angle X-ray scattering (WAXS). 2D WAXS data was collected using a Xenocs Xeuss 2.0 X-ray instrument operating with a  $\text{Cu K}\alpha$  source ( $\lambda = 1.54 \text{ \AA}$ ). Initially, 2D WAXS data (over a  $2\theta$  range of  $18\text{--}46^\circ$ ) was collected on a Pilatus 100 K detector system, which was calibrated with silver behenate. The WAXS detector was positioned in an evacuated chamber at a distance of 162 mm from the sample position. The cellulose samples were positioned vertically in the evacuated sample chamber, and the 2D WAXS was obtained with a data acquisition time of 120 s. Then, 2D WAXS data (over a  $2\theta$  range of  $10\text{--}34^\circ$ ) was collected on a Pilatus 300 K detector system (calibrated with silver behenate), at a sample-to-detector distance of 230 mm and a data acquisition time



of 300 s. All of the WAXS data was normalized for sample thickness, transmission, and background scattering. X-ray data reduction and analysis were performed using the Xeuss 2.0 instrument data processing and analysis software. The 2D WAXS data was reduced to 1D scattering profiles of intensity ( $I$ ) versus scattering angle  $2\theta$  by sector averaging around the beam stop by a fixed angle and radius.

The CI for BC and Whatman filter paper was estimated using the Segal method.<sup>31</sup> The height ratio between the (200) peak ( $I_{200}$ ) and the amorphous content intensity at  $2\theta = 18^\circ$  ( $I_{am}$ ) was determined, and the percentage of CI was then calculated by way of the following equation:

$$CI\% = \frac{I_{(200)} - I_{(am)}}{I_{(200)}} \times 100 \quad (1)$$

In addition to this, the crystallite size  $D$  (width), which is perpendicular to the (200) peak, was determined from the Scherrer equation:<sup>32</sup>

$$D(hkl) = \frac{0.9\lambda}{L \cos\theta} \quad (2)$$

where the  $\lambda$  is the X-ray wavelength,  $L$  is determined from the full width at half maximum (FWHM) determined from a Gaussian peak fit of the (200) peak, and  $\theta$  is the scattering angle.

### 3 | RESULTS AND DISCUSSION

#### 3.1 | Effect of cerato-platanin protein on the enzymatic hydrolysis of bacterial cellulose

Turbidity experiments were used to investigate the extent of the enzymatic hydrolysis of BC both in the presence and in the absence of CP. Previous work showed that a decrease in turbidity (i.e., an increase in transmittance) over time was a consequence of the size reduction of the BC fibrils down to the nanoscale level, which reduced the light scattering in the BC aqueous solution.<sup>25</sup> As shown in Figure 1a-d, the turbidity decreased (i.e., the transmittance increased) for all the enzyme/BC ratios until an apparent steady state was reached; this clearly demonstrates that the rate of the process decreased over time, which is a typical feature of cellulose hydrolysis.<sup>33</sup>

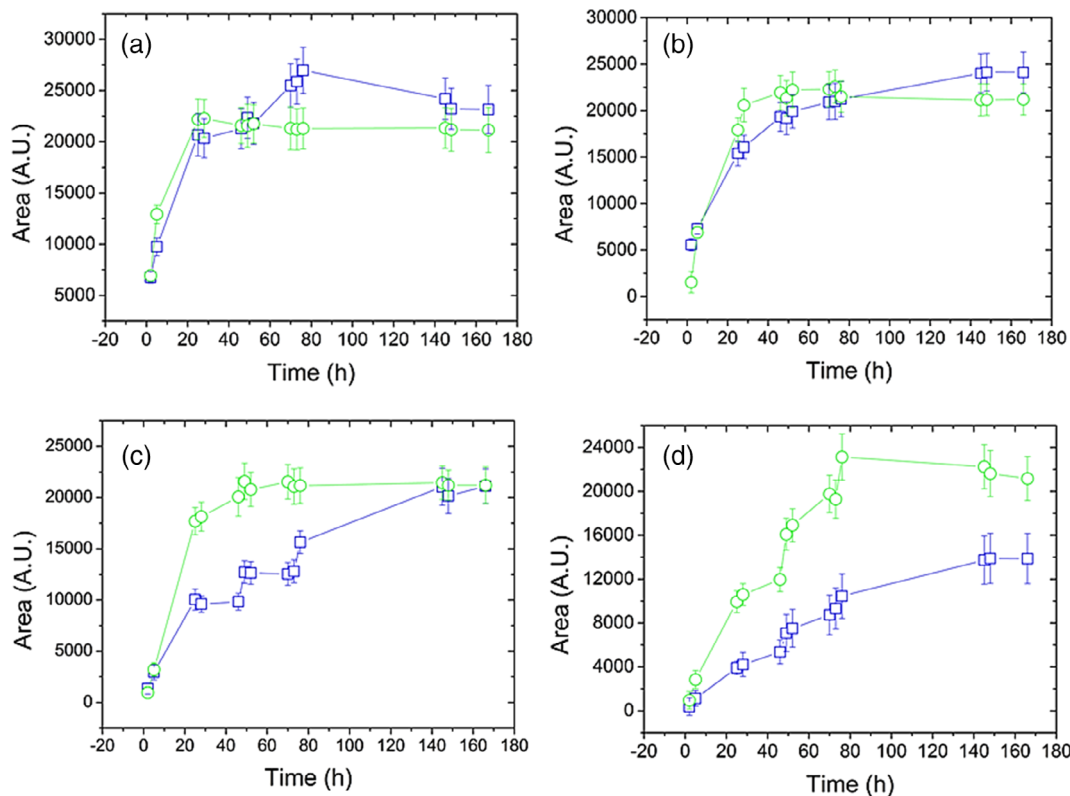


**FIGURE 1** Evolution of turbidity (expressed as the area under the transmittance spectra) during 166 h of hydrolysis for the enzyme/BC ratios 1:1 (a), 0.5:1 (b), 0.33:1 (c), and 0.25:1 (d), with (—□—) and without (—○—) cerato-platanin protein [Color figure can be viewed at [wileyonlinelibrary.com](http://wileyonlinelibrary.com)]

However, different patterns were detected among the transmittance-versus-time curves, depending on the enzyme concentration and the presence of CP in the hydrolytic reaction.

For the lowest enzyme/BC ratios (i.e., samples 1:1 and 0.5:1), the turbidity experiments led to a similar trend with and without the CP (Figure 1a,b). When the BC concentration increased further (samples 0.33:1 and 0.25:1), the spectrophotometric pattern changed greatly in the presence or absence of CP. More specifically, for sample 0.33:1 (Figure 1c), the addition of the non-catalytic protein on the overall hydrolysis process of BC yielded an apparent delay; that is, the kinetics of the hydrolytic reaction slowed down. Nevertheless, the final transmittance value (which is an indication of the overall extent of hydrolysis) was comparable between the two operating conditions (with or without CP).

When the amount of BC was brought to its maximum (i.e., enzyme/BC concentration = 0.25:1), two completely distinct curves were obtained in the presence or in the absence of CP. In particular, the transmittance values arising from the enzymatic hydrolysis in the presence of CP were located at lower levels throughout the investigated temporal window (166 h) (Figure 1d). Overall, the turbidity experiments suggest that the addition of CP did not bring any significant boosting effect on the hydrolysis process of the cellulosic substrate. Rather, it seemed to have an inhibitory effect for the highest enzyme/BC ratio (i.e., 0.25:1) while relenting the overall hydrolytic process for the enzyme/BC ratio 0.33:1. Quantitatively, this is clearly shown by the fact that, in both formulations of 0.33:1 and 0.25:1, the maximum enzymatic activity was reached after 49 and 76 h, respectively, in the absence of the non-catalytic protein. However, in the presence of CP, the maximum hydrolytic activity peak was centered at ~145 h in both samples.

The apparent inhibitory effect of CP can be plausibly explained in terms of both competition for the binding sites on the cellulose backbone and lack of affinity of CP toward the BC backbone. In other words, cellulase and

CP simultaneously attack the same sites displaced on cellulose molecules, with the CP hindering the enzymatic hydrolysis of cellulase because of steric hindrance. The fact that the inhibitory effect was observed for the lowest amounts of cellulase (0.25:1 and 0.33:1 formulations) seems to support the above considerations, that is, the limiting effect of CP was more intense when the competition for the binding sites on the BC backbone was lower. At the same time, CP did not play any activity on the BC skeleton. Under this scenario, the enzymatic hydrolysis rate mediated by cellulase clearly decreased and relented over time. This effect was not obvious for the formulations 1:1 and 0.5:1 probably because the much higher concentration of cellulase prevailed over the CP, limiting any possible inhibitory effect. Unfortunately, it has not been possible to support the above hypothesis by experimental evidence because the CP linkages with the bacterial cellulose binding sites are not stable, as also confirmed by a previous work on CP and plant cellulose.<sup>2,11,12,34</sup> Hence, the transient nature of the CP/BC interactions are very difficult to detect by conventional techniques, being real-time approaches more appropriate.

### 3.2 | Cellobiose and glucose quantification

The high-performance liquid chromatography (HPLC) analysis was used to determine the amount of cellobiose and glucose as final products of the enzymatic hydrolysis of BC. It is expected that the more effective the hydrolysis reaction, the higher the amount of cellobiose and glucose that will be produced. The results of the HPLC analysis are reported in Table 1. The concentrations of cellobiose and glucose varied oppositely as a function of the enzyme/BC ratio, both in the presence and absence of CP. More specifically, the disaccharide concentration decreased as the ratio increased, whereas the hexose concentration increased monotonically as the amount of

**TABLE 1** Cellobiose and glucose concentrations at the end of the hydrolytic reaction (166 h) of BC mediated by cellulase, in the presence and in the absence of CP protein for different enzyme/BC ratios. The results are expressed as mean values (standard deviations). Different superscripts (A, B, C, D, E, F, G, H) refer to statistically significant differences within and between groups ( $p < 0.05$ )

Formulation (cellulase/BC [w/w])	Cellobiose (g L <sup>-1</sup> )		Glucose (g L <sup>-1</sup> )	
	No CP protein	With CP protein	No CP protein	With CP protein
0.25:1	1.54 (± 0.04) <sup>A</sup>	1.15 (± 0.12) <sup>E</sup>	2.25 (± 0.12) <sup>A</sup>	1.48 (± 0.13) <sup>E</sup>
0.33:1	1.40 (± 0.04) <sup>B</sup>	1.03 (± 0.15) <sup>F</sup>	2.66 (± 0.04) <sup>B</sup>	2.15 (± 0.01) <sup>F</sup>
0.5:1	1.19 (± 0.03) <sup>C</sup>	0.81 (± 0.03) <sup>G</sup>	3.43 (± 0.12) <sup>C</sup>	2.58 (± 0.31) <sup>G</sup>
1:1	0.34 (± 0.02) <sup>D</sup>	0.29 (± 0.02) <sup>H</sup>	4.18 (± 0.23) <sup>D</sup>	2.95 (± 0.28) <sup>H</sup>

enzyme increased, confirming what was observed in a recent work.<sup>25</sup> In other words, while the concentration of cellobiose increased with the concentration of the cellulosic substrate (i.e., BC), the conversion of cellobiose into glucose by the  $\beta$ -glucosidases was higher for the mixtures that were richer in enzymes. In the presence of the non-catalytic protein, the concentration of both cellobiose and glucose was lower in comparison with the samples without CP for all the enzyme/BC ratios. This observation

supports the findings arising from the turbidity experiments; that is, the non-catalytic protein has an inhibitory effect on the enzymatic hydrolysis of BC probably due to a partial perturbation by steric hindrance of the linkage between cellulase and the  $\beta$ -1,4 binding site on the cellulosic backbone.

### 3.3 | Morphological characterization of bacterial cellulose nanocrystals

Particle-size analysis provided additional confirmation of the limiting role of the CP on the hydrolysis kinetics of BC mediated by cellulase. As depicted in Figure 2, a progressive reduction in size was observed as the enzyme/BC ratio increased (i.e., moving from the 0.25:1 formulation to the 1:1 formulation), both in the presence and in the absence of the non-catalytic protein. However, for all four enzyme/BC ratios, a clear shift toward lower sizes was observed for the formulations that did not include the CP.

For the highest enzyme concentration (formulation 1:1, Figure 2a),  $\sim 58\%$  of the hydrolysate had an average

**TABLE 2** Cellulase/BC mixture (w/w) with the related amount ( $\mu\text{g}$ ) of cellulase and corresponding enzymatic units (U)

Cellulase <sup>a</sup> /BC <sup>b</sup> (w/w)	Cellulase <sup>a</sup> ( $\mu\text{g}$ )	Enzyme unit (U)
0.25:1	28	1
0.33:1	37	2
0.5:1	56	3
1:1	113	4

<sup>a</sup>Prepared from a starting aqueous solution ( $5 \text{ mg g}^{-1}$ ; see main text for details).

<sup>b</sup>Prepared from a starting aqueous dispersion (12% by weight; see main text for details).

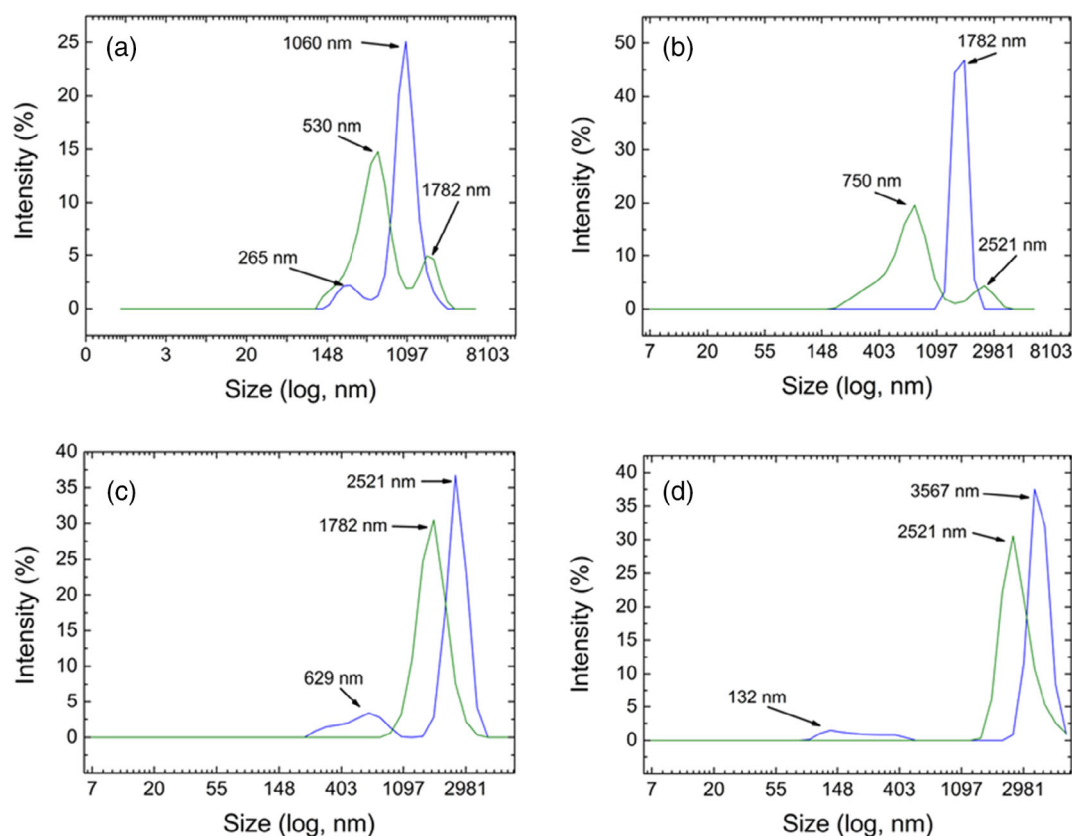


**FIGURE 2** Size-distribution intensity plot of hydrolyzed BC after 166 h, using dynamic light scattering, for the 1:1 (a), 0.5:1 (b), 0.33:1 (c), and 0.25:1 (d) enzyme/BC ratios, with (–) and without (–) the non-catalytic protein. The particle size at the main intensity peaks is also shown [Color figure can be viewed at [wileyonlinelibrary.com](http://wileyonlinelibrary.com)]

size within the range of 890 nm–1.26  $\mu\text{m}$  in the presence of CP, whereas this range decreased to 445–630 nm for  $\sim 40\%$  of the hydrolysate without CP. As the concentration of the enzyme decreased (formulation 0.5:1, Figure 2b), the above ranges increased to 1.5–2.12  $\mu\text{m}$  for  $\sim 97\%$  of the hydrolysate and 630–890 nm for  $\sim 50\%$  of the hydrolysate with and without CP, respectively. In the case of formulation 0.33:1 (Figure 2c),  $\sim 77\%$  of the hydrolysate had an average size within the range of 2.12–3  $\mu\text{m}$  in the presence of the CP and 1.5–2.12  $\mu\text{m}$  for  $\sim 75\%$  of the hydrolysate without CP. Finally, the lowest enzyme/BC ratio (formulation 0.25:1, Figure 2d) had an average size range of 3–4.24  $\mu\text{m}$  for  $\sim 82\%$  of the hydrolysate obtained in the presence of CP, whereas  $\sim 74\%$  of the hydrolysate obtained in the absence of CP was within the range of 2.12–3  $\mu\text{m}$ . It is also worth mentioning that the main peak of the particle size plot associated with the enzymatic hydrolysis of BC in the absence of CP was always broader compared to the main peak obtained for the formulations that included the non-catalytic protein. This observation confirmed that the enzymatic hydrolysis of BC is a heterogeneous process, giving rise to a large polydispersity of BC-derived nanoparticles.<sup>25</sup>

To corroborate the best performing reduction in size of BC without CP, both AFM and TEM images were collected (Figure 3). As shown in Figure 3a, in the presence of CP, longer fibers and entangled patches were observed, whereas needle-like morphologies (approaching those

typical for cellulose nanocrystals) were detected when the CP was not used (Figure 3b). TEM observations confirmed the same trend, with fibrous morphology and larger sizes (especially in terms of width) in the presence of CP (Figure 3c); thinner morphologies and individual nanocrystals were seen in the absence of CP (Figure 3d). These observations seem to suggest that the erosion of the BC fibers due to the enzymatic attack was less pronounced in the presence of CP, thus supporting the finding that the enzymatic attack was less effective when the CP was used. Both TEM and AFM images confirmed the dimensional shift detected by the DLS analysis, that is, the length of BCNCs varied proportionally depending on the enzymatic concentrations, both in the presence and in the absence of CP. For example, in the presence of the CP, the length of the BCNCs varied from  $\sim 1$  to  $\sim 3$   $\mu\text{m}$  ( $\sim 60$  nm width). On the opposite, without CP, the length of the BCNCs varied from  $\sim 0.8$  to  $\sim 2$   $\mu\text{m}$  ( $\sim 40$  nm width) for the 0.25:1 enzyme/BC ratio (Figure 3a,b). Similar results were also obtained by TEM analysis, whereby a mean width value of  $\sim 70$  and  $\sim 55$  nm was obtained with and without the presence of CP, respectively (Figure 3c,d), thus supporting the polydispersity of the BCNCs obtained by enzymatic hydrolysis.

### 3.4 | Possible explanation of the CP's behavior toward BC

It has been demonstrated that Cerato-platanins show increased enzymatic activity on plant cellulose and plant cellulose derivatives, such as filter paper<sup>9,10,12</sup> and carboxymethyl cellulose,<sup>10</sup> respectively. This effect was attributed to the expansin-like behavior of CPF members, which could loosen the cellulosic network in a non-catalytic manner, thus enhancing the attack of cellulases by making the cellulosic substrate more accessible. On the other hand, the same expansin-like behavior of Cerato-platanins was not observed on other polysaccharides such as chitin, 1,3- $\beta$ -glucan, xylan, and pectin.<sup>10</sup>

To gain a deeper understanding of the CP's behavior toward BC, we have compared BC with another cellulosic substrate as far as their structural properties are concerned. Among others, we selected Whatman grade 3MM filter paper as a control, because it shares some similarities with BC, being water insoluble and having high purity, high crystallinity, and the same chemical composition. Moreover, the Whatman filter paper was successfully used as a substrate to test the expansin-like activity of cerato-platanins.<sup>9,10,12</sup> Therefore, we performed 2D WAXS experiments on both the dried BC and filter paper.

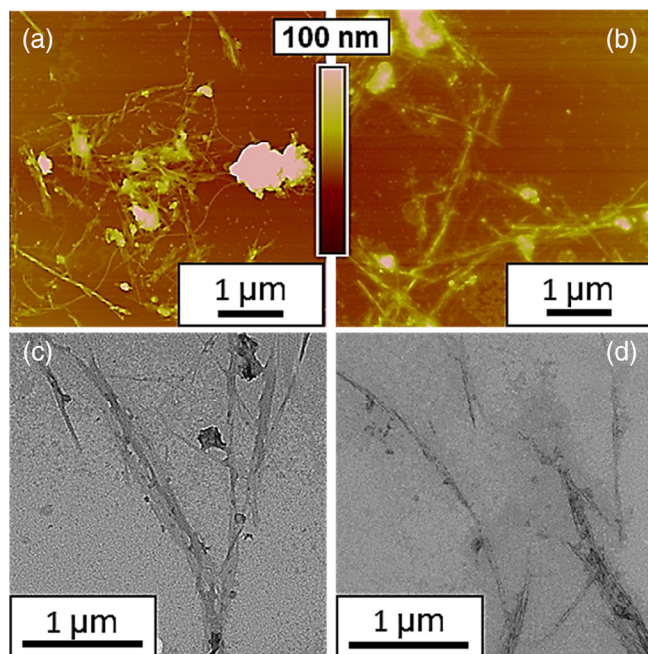
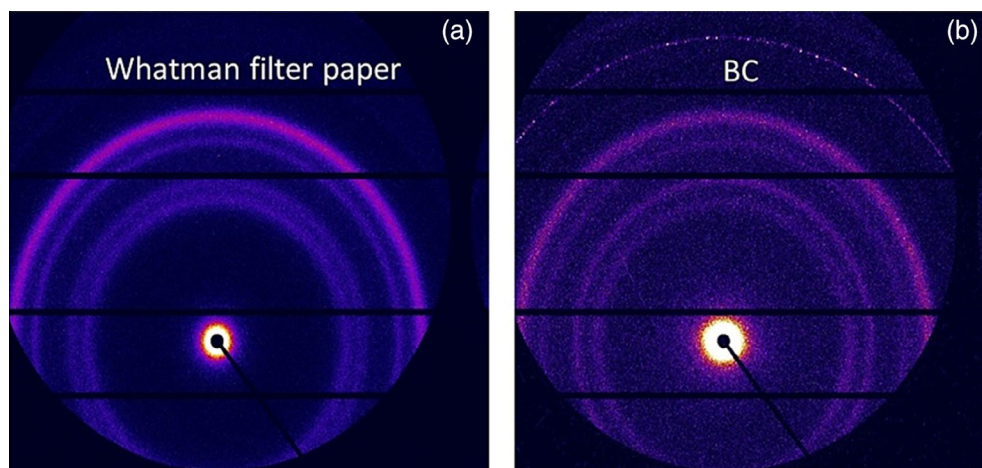


**FIGURE 3** AFM (a–b) height images and TEM (c–d) images of BC for the enzyme/BC ratio 0.25:1 after 166 h hydrolysis with (a,c) and without (b,d) cerato-platanin protein [Color figure can be viewed at [wileyonlinelibrary.com](http://wileyonlinelibrary.com)]



**FIGURE 4** 2D WAXS patterns of Whatman filter paper cellulose (a) and BC (b) [Color figure can be viewed at [wileyonlinelibrary.com](http://wileyonlinelibrary.com)]



To determine if the cellulose samples had any preferred orientation induced from processing, 2D WAXS patterns were obtained, which are shown in Figure 4. Here, the crystalline Bragg peaks are shown as complete rings in the WAXS patterns, indicating no preferred orientation of the cellulose fibers in either the Whatman filter paper or BC samples.

To further characterize the WAXS, 1D profiles were obtained from the 2D patterns, which are shown in Figure 5. The 1D WAXS profiles, although similar, exhibit some differences. In Figure 5a, the main peaks are indexed as (1-10), (110), (102), and (200), which are typical of the cellulose I polymorph in both samples.

The (102) peak is prominent in the 1D WAXS profiles, which is indicative of cellulose I with no preferred orientation, as established from the 2D WAXS in Figure 4.<sup>35</sup> These X-ray profiles were further compared with those calculated for cellulose I, which has two distinct crystalline forms; cellulose I $\alpha$  (triclinic), the dominant form in bacteria, and cellulose I $\beta$  (monoclinic),<sup>36,37</sup> a predominant polymorph present in higher plants. The two peaks centered at 15° (1-10) and 16.6° (110) in the filter paper profile are attributed to the cellulose I $\beta$  crystal form. These peaks shift toward slightly lower and higher angles, respectively, in the BC pattern (Figure 5a), and are attributed to the cellulose I $\alpha$ .<sup>35,36</sup> In addition, the peak at 35.4°, again characteristic of the crystal form of cellulose I, is visible in both 1D profiles but is weaker in the BC profile (Figure 5b).<sup>35</sup> It should also be noted that the 1D X-ray profile of BC (Figure 5a) exhibited two unexpected peaks at 29° and 32.5°. In consideration of the production process of BC and excluding any external contamination, we are prone to associate these peaks to residues of NaOH crystals used to remove the cells of *Komagataeibacter sucrofermentans* from the cellulose mat obtained after the fermentation.

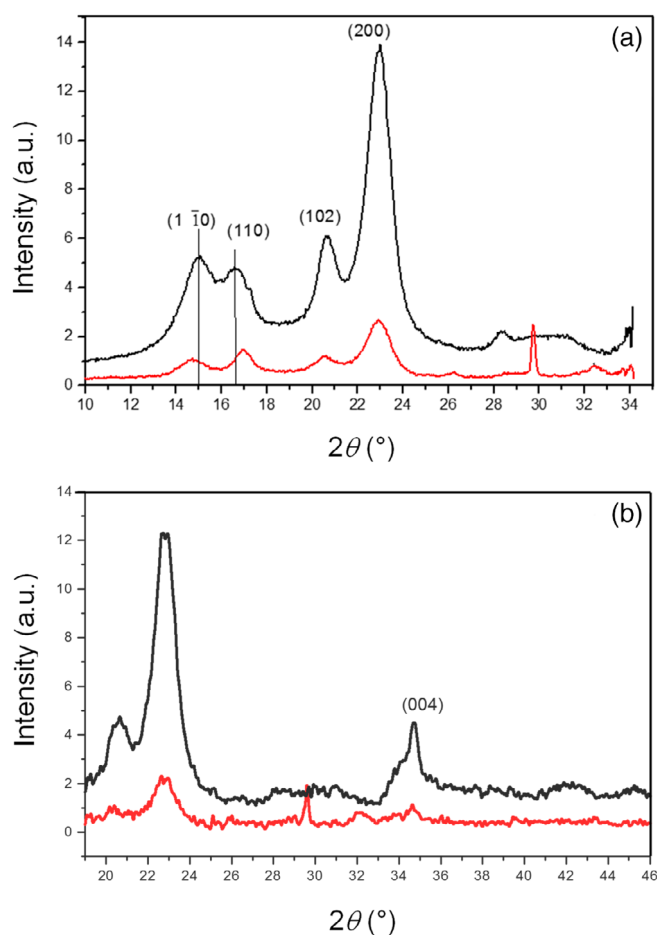


**FIGURE 5** 1D WAXS diffraction patterns of BC (—) and Whatman filter paper (—) in the  $2\theta$  range of 10°–34° (a) and 19°–46° (b) (miller indices are reported between parentheses) [Color figure can be viewed at [wileyonlinelibrary.com](http://wileyonlinelibrary.com)]

A quantitative analysis of the 1D X-ray profiles gives information on the crystallite size and crystallinity index (CI), which are important properties to consider in cellulose applications such as enzyme digestibility.<sup>36</sup> The CI

values (calculated via Equation 1), for the filter paper and BC were 81% and 75%, respectively. Similarly, the crystallite size (calculated using Equation 2) for the filter paper and BC were 6.8 and 6.6 nm, respectively. The crystallinity and crystallite size of the filter paper was high because it was made from cotton linters, which is one of the purest forms of cellulose.<sup>38</sup> BC cellulose is also known to have a high crystallinity and crystal size, so the results are in accordance with other reports on these types of cellulose.<sup>38,39</sup>

The two polymorphs of cellulose I have two varying lattice structures and different hydrogen bonding patterns, which governs the stability and properties of these polymorphs.<sup>39</sup> Therefore, a first consequence is that such different structural features might have played a role in the lack of activity of the CP in the presence of BC, probably due to lack of affinity of the protein for the BC binding sites. In this regard, the most accredited hypothesis related to the mechanism of action of expansins-like protein, consists in the destruction of hydrogen bonds between cellulose polymers.<sup>2</sup> Our findings suggest that the activity of CPF members seems to depend not only on the type of cellulosic substrate, but also on the structural features of molecules with the same chemical composition, that is, polysaccharide-based structures. Moreover, divergence in hydrogen bonds conformation between bacterial and Whatman filter paper (i.e., plant-derived) celluloses, could be explained in term of different CP activity on these substrates. As mentioned above, the action mechanism of expansin-like cerato-platanin (CP) protein indwelled in the shattering of hydrogen bonds between cellulose polymers.<sup>2</sup> The intimate biochemistry/chemistry reasons, however, should be further elucidated.

## 4 | CONCLUSIONS

Enzymatic hydrolysis of cellulose attracts increasing interest not only for the production of bioethanol but also for more recent uses, such as obtaining cellulose nanoparticles (i.e., cellulose nanocrystals) that can be used as reinforcing agents for a wide range of materials and applications.

In this work, the expansin-like activity of CP during the enzymatic hydrolysis of BC was investigated. We found that CP did not play an enhancing effect on the hydrolytic activity of cellulases by *Trichoderma reesei*. Rather, at the lowest enzyme/BC ratios, the simultaneous presence of the CP protein in the formulation seemed to hinder the activity of the cellulases, probably due to a competition for the binding sites on the cellulose backbone and lack of affinity of the protein for BC. This anomalous behavior, in comparison with the successful activity

of cerato-platanins on plant cellulose, has never been described before. It has been plausibly explained in terms of structural differences between BC and cellulose from plants, although further investigation is necessary to clarify the biochemistry/chemistry reasons in depth.

The lack of any hydrolytic activity of these proteins on BC confirms that BC shows unique physiochemical properties compared to plant cellulose. BC has been recently proposed for a large variety of applications, from skin repair treatments in cases of burns, wounds, and ulcers to food packaging developments.<sup>40,41</sup> As a model for other expansin-like proteins produced by pathogenic fungi that can be recovered in foods or wounds, the absence of loosening activity on BC adds a positive feature to the potential functionalities of polymers based on BC.

## ACKNOWLEDGMENTS

The authors acknowledge Dr Steve Huband for SAXS/WAXS data collection and processing at the University of Warwick, UK. Open Access Funding provided by Universita degli Studi di Firenze within the CRUI-CARE Agreement.

## CONFLICT OF INTEREST

The authors declare no potential conflict of interest.

## AUTHOR CONTRIBUTION

Cesare Rovera, Simone Luti, and Stefano Farris conceived the experiments; Diego Romano dealt with the BC production and conducted the HPLC analysis; Cesare Rovera dealt with the BCNCs production and carried out BCNCs characterization. Ellen L. Heeley and Chaoying Wan performed the X-ray diffraction analysis; Simone Luti and Luigia Pazzagli took care of the production of CP. Cesare Rovera and Stefano Farris assembled the figures for the final manuscript. Cesare Rovera, Simone Luti, and Stefano Farris wrote the main manuscript text, which was completed by all the authors. Stefano Farris acquired the funds.

## DATA AVAILABILITY STATEMENT

The data that support the findings of this study are available from the corresponding author upon reasonable request.

## ORCID

Cesare Rovera  <https://orcid.org/0000-0002-3595-8564>

Simone Luti  <https://orcid.org/0000-0001-7050-6590>

Luigia Pazzagli  <https://orcid.org/0000-0002-6365-1615>

Ellen L. Heeley  <https://orcid.org/0000-0002-2803-7492>

Chaoying Wan  <https://orcid.org/0000-0002-1079-5885>

Diego Romano  <https://orcid.org/0000-0002-2448-1692>

Stefano Farris  <https://orcid.org/0000-0002-6423-8443>

## REFERENCES

- [1] L. Pazzagli, G. Cappugi, G. Manao, G. Camici, A. Santini, A. Scala, *J. Biol. Chem.* **1999**, 274, 24959.
- [2] S. Luti, L. Sella, A. Quarantin, L. Pazzagli, I. Baccelli, *Fungal Biol. Rev.* **2020**, 34, 13.
- [3] E. V. Gomes, M. Costa, R. G. De Paula, R. Ricci de Azevedo, F. L. Da Silva, E. F. Noronha, C. José Ulhoa, V. Neves Monteiro, R. Elena Cardoza, S. Gutiérrez, R. Nascimento Silva, *Sci. Rep.* **2016**, 5, 17998.
- [4] N. M. R. Ashwin, L. Barnabas, A. Ramesh Sundar, P. Malathi, R. Viswanathan, A. Masi, G. K. Agrawal, R. Rakwal, *J. Proteomics* **2017**, 169, 2.
- [5] I. Baccelli, *Front. Plant Sci.* **2015**, 5, 1.
- [6] L. Pazzagli, V. Seidl-Seiboth, M. Barsottini, W. A. Vargas, A. Scala, P. K. Mukherjee, *Plant Sci.* **2014**, 228, 79.
- [7] A. L. De Oliveira, M. Gallo, L. Pazzagli, C. E. Benedetti, G. Cappugi, A. Scala, B. Pantera, A. Spisni, T. A. Pertinhez, D. O. Cicero, *J. Biol. Chem.* **2011**, 286, 17560.
- [8] M. R. De Barsottini, J. F. De Oliveira, D. Adamoski, P. J. P. L. Teixeira, P. F. V. Do Prado, H. O. Tiezzi, M. L. Sforça, A. Cassago, R. V. Portugal, P. S. L. De Oliveira, A. C. De M. Zeri, S. M. G. Dias, G. A. G. Pereira, A. L. B. Ambrosio, *Mol. Plant-Microbe Interact.* **2013**, 26, 1281.
- [9] I. Baccelli, S. Luti, R. Bernardi, A. Scala, L. Pazzagli, *Appl. Microbiol. Biotechnol.* **2014**, 98, 175.
- [10] A. Quarantin, C. Castiglioni, W. Schäfer, F. Favaron, L. Sella, *Plant Physiol. Biochem.* **2019**, 139, 229.
- [11] S. Luti, F. Martellini, F. Bemporad, L. Mazzoli, P. Paoli, L. Pazzagli, *PLoS One* **2017**, 12, e0178337.
- [12] S. Luti, F. Bemporad, M. Vivoli Vega, M. Leri, F. Musiani, I. Baccelli, L. Pazzagli, *Int. J. Biol. Macromol.* **2020**, 165, 2845.
- [13] A. Pennacchio, R. Pitocchi, G. C. Varese, P. Giardina, A. Piscitelli, *Microb. Biotechnol.* **2021**, 14, 1699.
- [14] Y. Yamada, P. Yukphan, H. T. Lan Vu, Y. Muramatsu, D. Ochaikul, S. Tanasupawat, Y. Nakagawa, *J. Gen. Appl. Microbiol.* **2012**, 58, 397.
- [15] H. M. C. Azeredo, H. Barud, C. S. Farinas, V. M. Vasconcellos, A. M. Claro, *Front. Sustainable Food Syst.* **2019**, 3, 1.
- [16] Q. Fang, X. Zhou, W. Deng, Z. Zheng, Z. Liu, *Sci. Rep.* **2016**, 6, 33185.
- [17] Y.-C. Hsieh, H. Yano, M. Nogi, S. J. Eichhorn, *Cellulose* **2008**, 15, 507.
- [18] S. Reiling, J. Brickmann, *Macromol. Theory Simul.* **1995**, 4, 725.
- [19] G. Guhados, W. Wan, J. L. Hutter, *Langmuir* **2005**, 21, 6642.
- [20] M. Rollini, A. Musatti, D. Cavicchioli, D. Bussini, S. Farris, C. Rovera, D. Romano, S. De Benedetti, A. Barbiroli, *Sci. Rep.* **2020**, 10, 21358.
- [21] K. J. Nagarajan, N. R. Ramanujam, M. R. Sanjay, S. Siengchin, B. Surya Rajan, K. Sathick Basha, P. Madhu, G. R. Raghav, *Polym. Compos.* **2021**, 42, 1588.
- [22] W. J. Lee, A. J. Clancy, E. Kontturi, A. Bismarck, M. S. P. Shaffer, *ACS Appl. Mater. Interfaces* **2016**, 8, 31500.
- [23] J. Araki, M. Wada, S. Kuga, *Langmuir* **2001**, 17, 21.
- [24] P. Lu, Y.-L. Hsieh, *Carbohydr. Polym.* **2010**, 82, 329.
- [25] C. Rovera, M. Ghaani, N. Santo, S. Trabattoni, R. T. Olsson, D. Romano, S. Farris, *ACS Sustainable Chem. Eng.* **2018**, 6, 7725.
- [26] Y. Zheng, Z. R. Pan Zhongli, *Int. J. Agric. Biol. Eng.* **2009**, 2, 21.
- [27] M. Hall, P. Bansal, J. H. Lee, M. J. Realff, A. S. Bommarius, *Bioresour. Technol.* **2011**, 102, 2910.
- [28] W. Wang, T. Yuan, K. Wang, B. Cui, Y. Dai, *Bioresour. Technol.* **2012**, 107, 282.
- [29] R. Sindhu, P. Binod, A. Pandey, *Bioresour. Technol.* **2016**, 199, 76.
- [30] S. Luti, A. Caselli, C. Taiti, N. Bazihizina, C. Gonnelli, S. Mancuso, L. Pazzagli, *Int. J. Mol. Sci.* **2016**, 17, 866.
- [31] L. Segal, J. J. Creely, A. E. Martin, C. M. Conrad, *Text. Res. J.* **1959**, 29, 786.
- [32] A. L. Patterson, *Phys. Rev.* **1939**, 56, 978.
- [33] P. Valjamae, V. Sild, A. Nutt, G. Pettersson, G. Johansson, *Eur. J. Biochem.* **1999**, 266, 327.
- [34] R. Gaderer, K. Bonazza, V. Seidl-Seiboth, *Appl. Microbiol. Biotechnol.* **2014**, 98, 4795.
- [35] S. Nam, A. D. French, B. D. Condon, M. Concha, *Carbohydr. Polym.* **2016**, 135, 1.
- [36] Z. Ling, S. Chen, X. Zhang, K. Takabe, F. Xu, *Sci. Rep.* **2017**, 7, 10230.
- [37] A. D. French, *Cellulose* **2014**, 21, 885.
- [38] K. Leppänen, S. Andersson, M. Torkkeli, M. Knaapila, N. Kotelnikova, R. Serimaa, *Cellulose* **2009**, 16, 999.
- [39] R. J. Moon, A. Martini, J. Nairn, J. Simonsen, J. Youngblood, *Chem. Soc. Rev.* **2011**, 40, 3941.
- [40] A. F. Jozala, L. C. De Lencastre-Novaes, A. M. Lopes, V. De Carvalho Santos-Ebinuma, P. G. Mazzola, A. Pessoa-Jr, D. Grotto, M. Gerenutti, M. V. Chaud, *Appl. Microbiol. Biotechnol.* **2016**, 100, 2063.
- [41] Y. Huang, C. Zhu, J. Yang, Y. Nie, C. Chen, D. Sun, *Cellulose* **2014**, 21, 1.

**How to cite this article:** C. Rovera, S. Luti, L. Pazzagli, E. L. Heeley, C. Wan, D. Romano, S. Farris, *J. Appl. Polym. Sci.* **2021**, e51886. <https://doi.org/10.1002/app.51886>